Trafficking of the human ether-a-go-go-related gene (hERG) potassium channel is regulated by the ubiquitin ligase rififylin (RFFL)

Received for publication, May 7, 2018, and in revised form, October 17, 2018 Published, Papers in Press, November 6, 2018, DOI 10.1074/jbc.RA118.003852

Karim Roder[‡1], Anatoli Kabakov[‡1], Karni S. Moshal[‡], Kevin R. Murphy[‡], An Xie[§], Samuel Dudley[§], Nilüfer N. Turan[‡], Yichun Lu[‡], Calum A. MacRae[¶], and Gideon Koren[‡2]

From the [‡]Department of Medicine, Division of Cardiology, Cardiovascular Research Center, Rhode Island Hospital, The Warren Alpert Medical School of Brown University, Providence, Rhode Island 02903, the [§]Department of Medicine, University of Minnesota, Cardiovascular Division, Minneapolis, Minnesota 55455, and the [¶]Cardiovascular Division, Brigham and Women's Hospital, Harvard Medical School, Boston, Massachusetts 02115

Edited by George N. DeMartino

The QT interval is an important diagnostic feature on surface electrocardiograms because it reflects the duration of the ventricular action potential. A previous genome-wide association study has reported a significant linkage between a single-nucleotide polymorphism ~11.7 kb downstream of the gene encoding the RING finger ubiquitin ligase rififylin (RFFL) and variability in the QT interval. This, along with results in animal studies, suggests that RFFL may have effects on cardiac repolarization. Here, we sought to determine the role of RFFL in cardiac electrophysiology. Adult rabbit cardiomyocytes with adenovirus-expressed RFFL exhibited reduced rapid delayed rectifier current (I_{Kr}). Neonatal rabbit cardiomyocytes transduced with RFFL-expressing adenovirus exhibited reduced total expression of the potassium channel ether-a-go-go-related gene (rbERG). Using transfections of 293A cells and Western blotting experiments, we observed that RFFL and the core-glycosylated form of the human ether-a-go-go-related gene (hERG) potassium channel interact. Furthermore, RFFL overexpression led to increased polyubiquitination and proteasomal degradation of hERG protein and to an almost complete disappearance of I_{Kr}, which depended on the intact RING domain of RFFL. Blocking the ER-associated degradation (ERAD) pathway with a dominant-negative form of the ERAD core component, valosin-containing protein (VCP), in 293A cells partially abolished RFFL-mediated hERG degradation. We further substantiated the link between RFFL and ERAD by showing an interaction between RFFL and VCP *in vitro*. We conclude that RFFL is an important regulator of voltage-gated hERG potassium channel activity and therefore cardiac repolarization and that this ubiquitination-mediated regulation requires parts of the ERAD pathway.

The QT interval measures the time from the beginning of the QRS complex to the end of the T wave on a surface electrocardiogram (1, 2) and reflects ventricular action potential duration (3). A prolonged QT interval increases the likelihood for polymorphous ventricular arrhythmias, which may lead to palpitations, dizziness, and sudden cardiac arrest in the general population (4, 5). As approximately one-third of QT interval variability is heritable (6–8), a number of genome-wide association studies have been performed to identify genes underlying this variation (9–12). For example, two genome-wide association studies (10, 11) of QT intervals identified two genetic variants downstream of the Ring finger and FYVE-like domain E3 ubiquitin protein ligase (*RFFL*)[3] gene, *viz.* rs2074518 and rs1052536, which are associated with modest changes in QT interval duration. Interestingly, a recent investigation by Joe and colleagues (13) used a congenic strain of Dahl salt-sensitive rats introgressed with genomic segments from the normotensive Lewis rat to map a quantitative trait locus for hypertension, short-QT interval, and cardiac hypertrophy to a 42.5-kb region that contains a single gene, *RFFL*. Although the authors speculated that, due to increased RFFL levels in the congenic rats, perturbations in endosomal recycling could be the underlying cause, no mechanistic studies were available. Human RFFL, a member of the RING finger ubiquitin ligases (14), encodes a 363-amino acid protein, which is widely expressed. It contains an N-terminal FYVE (Fab1, YOTB/ZK632.12, Vac1 and EEA1)-like domain similar to the phosphatidylinositol 3-phosphate–binding FYVE finger and a C-terminal RING finger required for its ubiquitin ligase activity (15, 16). In a number of *in vitro*

This work was supported by NHLBI, National Institutes of Health, Grants R01HL134706, R01HL110791, and R01HL046005 (to G. K.) and by the Rhode Island Foundation, Grant 20164378 (to K. S. M.). The authors declare that they have no conflicts of interest with the contents of this article. The content is solely the responsibility of the authors and does not necessarily represent the official views of the National Institutes of Health.

[1] Both authors contributed equally to the results of this work.

[2] To whom correspondence should be addressed: Rhode Island Hospital, The Warren Alpert Medical School of Brown University, 1 Hoppin St., Providence, RI 02903. Tel.: 401-444-4629; E-mail: gideon_koren@brown.edu.

[3] The abbreviations used are: RFFL, RING finger and FYFE-like domain-containing protein; APD, action potential duration; ARbCM, adult rabbit cardiomyocytes; CFTR, cystic fibrosis transmembrane conductance regulator; co-IP, co-immunoprecipitation; EGFP, enhanced green fluorescent protein; eQTL, expression quantitative trait loci; ER, endoplasmic reticulum; ERAD, ER-associated degradation; ERC, endocytic recycling compartment; ERQC, ER quality control; GTEx, Genotype-Tissue Expression; FYVE, Fab1, YOTB/ZK632.12, Vac1 and EEA1; HEK, human embryonic kidney; hERG, human ether-a-go-go-related gene; HP, holding potential; LIG3, DNA ligase 3; m.o.i., multiplicity of infection; NRbCM, neonatal rabbit cardiomyocytes; rbERG, rabbit ether-a-go-go-related gene; RNF207, Ring finger protein 207; SNP, single nucleotide polymorphism; VCP, valosin-containing protein; HA, hemagglutinin; GAPDH, glyceraldehyde-3-phosphate dehydrogenase; mTOR, mechanistic target of rapamycin.

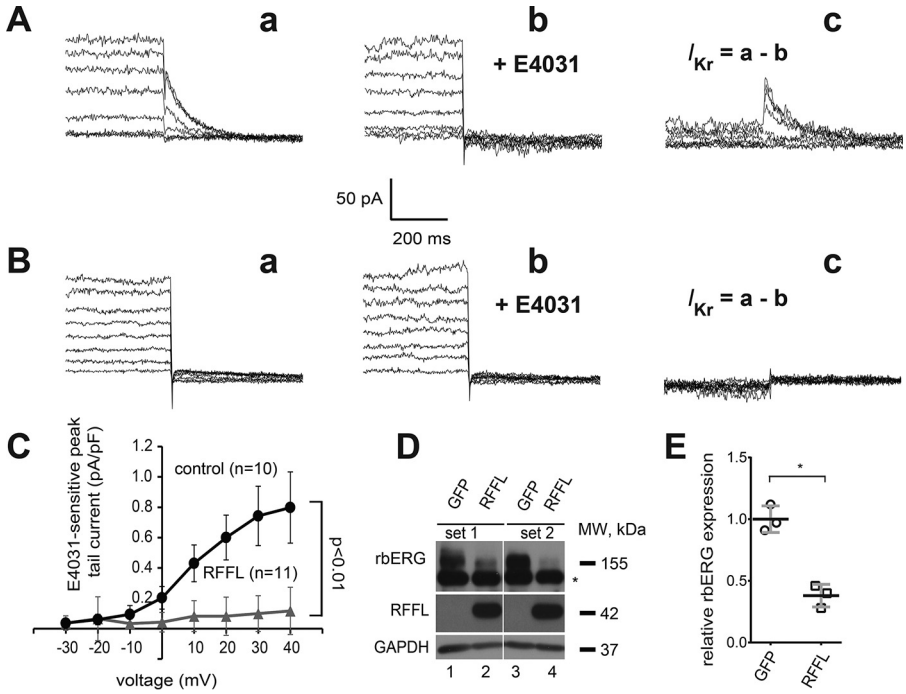

Figure 1. Overexpressed RFFL down-regulates I_{Kr} in adult rabbit cardiomyocytes. ARbCM were transduced with adenovirus encoding GFP (control) or RFFL (100 m.o.i., 48 h). *A*, representative current traces in GFP-expressing ARbCM. After a recording in control solution (*a*), the cells were perfused with 5 μM E-4031 (*b*) and I_{Kr} was defined as the difference, *i.e.* as E4031-sensitive current (*c*). HP was −40 mV and 3-s depolarizing test pulses were applied in 10-mV increments to maximum membrane potential of +40 mV. Displayed time period corresponds to the end of the depolarizing steps and the beginning of repolarization to HP, which is associated with I_{Kr} tail current. *B*, representative current traces in RFFL-expressing ARbCM. *C*, I-V curves of the peaks of E-4031-sensitive I_{Kr} tail currents (data are presented as mean ± S.D.) of GFP- or RFFL-transduced ARbCM ($p < 0.01$ in two-way analysis of variance; control and RFFL: cells from 6 animals each). *D*, NRbCM were infected with adenovirus encoding GFP (control) or RFFL (1 m.o.i., 48 h). Western blotting data were from NRbCM extracts to measure expression of rbERG, RFFL, and GAPDH (the *asterisk* indicates an unspecific band). *E*, respective relative expression levels of 155 kDa rbERG normalized to GAPDH expression from three independent experiments performed in triplicate (*, $p < 0.05$). In the scatter plot, averaged values for the three independent experiments together with the mean ± S.D. values are shown.

studies, RFFL has been linked to endocytic recycling, which requires an intact FYVE-like domain (15), p53 turnover through regulation of Mdm2 stability (17), tumor necrosis factor-induced NF-κB activation (18), and destabilization of PRR5L, a suppressor of mTORC2, resulting in mTORC2-mediated protein kinase Cδ phosphorylation and cell migration downstream of $G\alpha_{12}$ (19).

The aforementioned *RFFL*-proximal single nucleotide polymorphisms (SNPs) associated with modest changes in the QT interval duration in humans and the effect of elevated RFFL on the QT interval in a congenic rat strain prompted us to study the effect of RFFL on cardiac repolarization. We hypothesized that RFFL potentially acts through ubiquitination to alter ion channel synthesis, trafficking, and/or recycling or degradation through proteasomes or lysosomes (20). We therefore set out to identify RFFL-associated ion channels responsible for these effects. Here, we present data that support a role for RFFL in the regulation of human ether-a-go-go-related gene (hERG) forward trafficking, thereby affecting cardiac repolarization.

Results

RFFL negatively affects I_{Kr} expression in adult rabbit cardiomyocytes and lowers rabbit ether-a-go-go-related gene (rbERG) expression in neonatal rabbit cardiomyocytes

To evaluate the role of RFFL in the control of native I_{Kr}, we utilized ARbCM. After 48 h in culture, these cells generally show low but significant expression of E-4031–sensitive current I_{Kr} (21, 22). For the electrophysiological studies, cardiomyocytes were transduced with adenovirus encoding GFP or FLAG-RFFL for 48 h. We observed that the I_{Kr} peak tail current after the +40 mV depolarizing pulse was 0.80 ± 0.24 pA/pF in GFP-transduced ARbCM ($n = 10$), whereas it was significantly lower (0.12 ± 0.16 pA/pF, $p < 0.01$) in RFFL-transduced ARbCM ($n = 11$, Fig. 1, *A–C*). Due to remodeling of ARbCM in culture, we were unable to consistently detect rabbit ERG in immunoblots (data not shown). To see any possible effect of RFFL on rbERG expression, we therefore used adenovirally transduced neonatal rabbit cardiomyocytes, which show high expression of rbERG (23). We noticed that RFFL overexpression significantly reduced rbERG levels (155-kDa band) by ~60% in NRbCM (Fig. 1, *D* and *E*).

RFFL lowers hERG expression and function in 293A cells

To delineate the RFFL-dependent regulation of I_{Kr}, we switched to 293A cells transiently expressing hERG. Similar to the I_{Kr} data in adult cardiomyocytes (Fig. 1, *A–C*), RFFL expression resulted in an almost complete loss of hERG tail current (*e.g.* peak tail current following activation at 40 mV: 29.0 ± 10.9 pA/pF for control, and 0.4 ± 0.6 pA/pF for RFFL; $p < 0.05$; Fig. 2, *A* and *B*) in 293A cells. This was accompanied by a severe down-regulation of total hERG protein expression (Fig. 2, *C* and *G*). However, the ubiquitination-deficient ΔRING deletion of RFFL did not significantly change I_{Kr} (Fig. 2, *A* and *B*) or total hERG (Fig. 2, *C* and *G*).

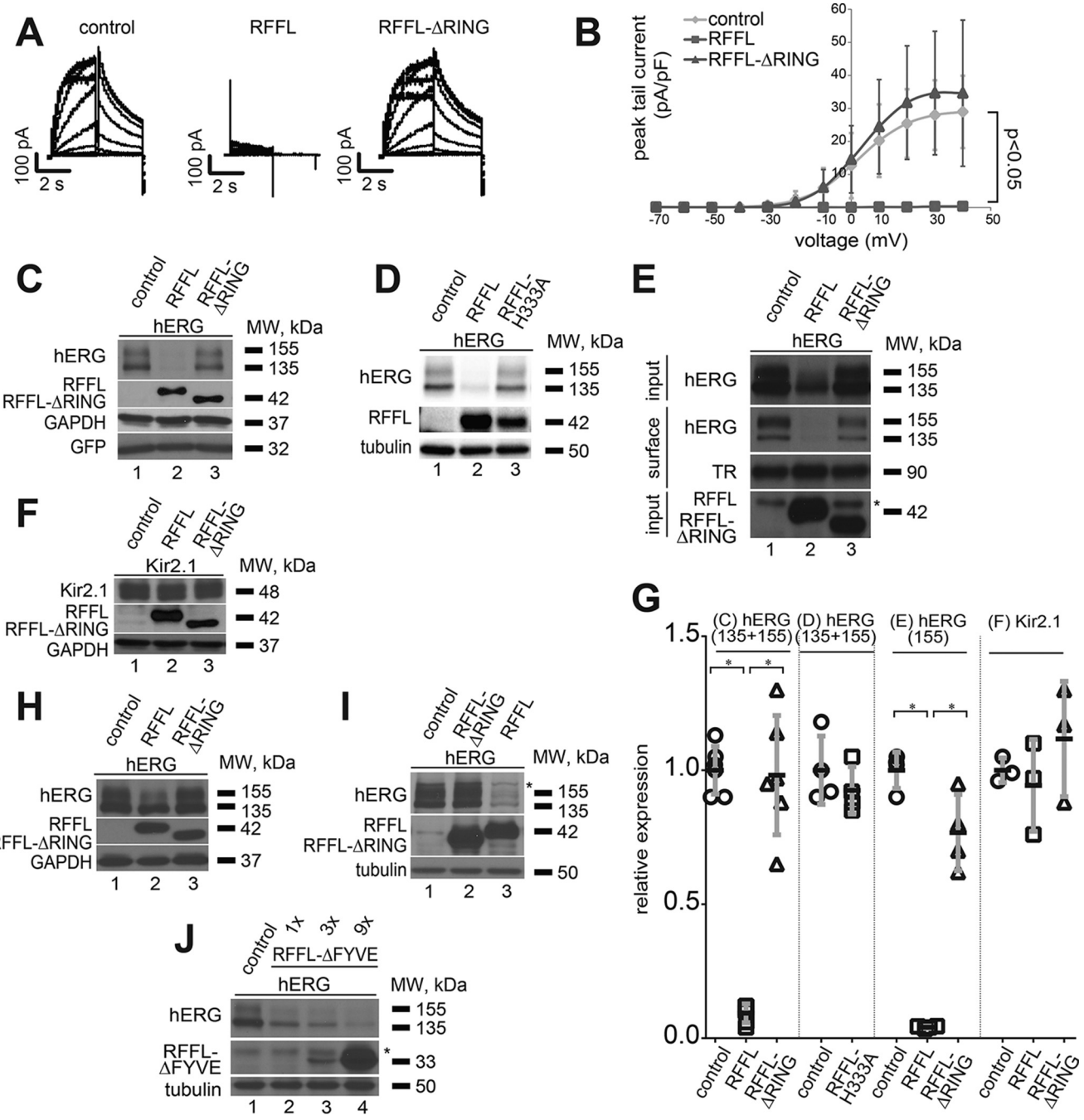

Figure 2. Overexpressed RFFL down-regulates I_{Kr} and hERG protein in 293A cells. 293A cells were co-transfected with GFP, hERG, and RFFL (WT and RING deletion) expression plasmids or control. *A*, representative traces of hERG currents from control, RFFL, and RFFL-ΔRING-expressing cells (HP = −80 mV). Voltage steps between −70 mV and 40 mV were applied to activate hERG channels before returning to −60 mV to record the tail currents. *B*, peak tail current amplitudes at −60 mV were normalized to cell capacitance. Data in the I-V curves are presented as mean ± S.D. (three independent experiments). The I_{Kr} peak tail current was almost completely abolished by RFFL expression ($p < 0.05$). *C*, respective total hERG expression levels in co-transfected 293A cells. *D*, 293A cells were transfected with hERG (*lanes 1-3*), pcDNA3 (*1*), RFFL (*2*), and RFFL-H333A plasmids (*3*). Respective total hERG expression levels are shown. *E*, 293A cells were transfected with hERG (*lanes 1–3*), pcDNA3 as control (*1*), FLAG-tagged RFFL (*2*), and RFFL-ΔRING plasmids (*3*). Cell-surface proteins were biotinylated using sulfo-NHS-SS-biotin, purified with neutravidin beads from total cell lysates, subjected to SDS-PAGE and blotted onto a nitrocellulose membrane. A representative immunoblot shows cell-surface (*surface*) and/or total (*input*) expression of hERG, transferrin receptor (*TR*), or GAPDH. FLAG antibody was used to detect total expression of RFFL and RFFL-ΔRING (the *asterisk* indicates an unspecific band). *F*, total Kir2.1 expression in 293A cells transiently co-transfected with plasmids encoding Kir2.1 (*lanes 1–3*), pcDNA3 (*1*) RFFL (*2*), and RFFL-ΔRING (*3*). *G*, respective relative expression levels (± S.D.) of total hERG expression (135- and 155-kDa bands) normalized to GAPDH or tubulin expression (*cf. panels C* and *D*), surface expression of hERG (155-kDa band) normalized to transferrin receptor expression (cf. *panel E*), and total Kir2.1 expression normalized to GAPDH expression (*cf. panel F*). In the scatter plot, averaged values for each independent experiment together with the mean ± S.D. values are shown (three to six independent experiments performed in triplicate each) (*, $p < 0.05$)). *H*, a representative Western blotting depicts total hERG expression in HEK cells with stable hERG expression (25), transiently transfected with plasmids encoding pcDNA3 (*1*), RFFL (*2*), and RFFL-ΔRING (*3*). *I*, a representative immunoblot shows total hERG expression in human osteosarcoma U-2 OS cells transiently co-transfected with plasmids encoding hERG (*lanes 1–3*), pcDNA3 (*1*), RFFL (*2*), and RFFL-ΔRING (*3*) (the *asterisk* indicates an unspecific band). *J*, total hERG expression in 293A cells transiently co-transfected with plasmids encoding hERG (*lanes 1–4*) and pcDNA (control; *lane 1*) along with increasing amounts of expression plasmid for RFFL-ΔFYFE (1, 3, and 9× molar ratio between RFFL-ΔFYFE and hERG expression plasmids; *lanes 2-4*) (the *asterisk* indicates an unspecific band).

Similarly, the ubiquitination-deficient mutant RFFL-H333A (the zinc-coordinating histidine of the RING domain Cys-X_2-Cys-X_{11}-Cys-X_1-His-X_3-Cys-X_2-Cys-X_6-Cys-X_2-Cys was replaced with alanine) (18, 24) had no effect on hERG expression (Fig. 2, *D* and *G*). These findings underscore the importance of a functional RING domain for an RFFL-dependent effect on hERG and I_{Kr}. Biotinylation of surface protein from co-transfected 293A cells indicated that expression of RFFL led to an approximate 90% decrease in hERG protein on the membrane (Fig. 2, *E* and *G*). The specificity of RFFL for hERG was further supported by the finding that levels of the co-expressed inward-rectifier potassium channel Kir2.1 were not affected by WT RFFL or RFFL-ΔRING in 293A cells (Fig. 2, *F* and *G*). Down-regulation of total hERG levels upon expression of RFFL, which required an intact RING domain, was also seen in HEK cells stably expressing hERG (25) (Fig. 2*H*) and human osteosarcoma U-2 OS cells transiently co-transfected (Fig. 2*I*). Previously, Coumailleau and colleagues (15) demonstrated that overexpressed RFFL was localized to the endocytic recycling compartment (ERC) and delayed transferrin recycling from the ERC to the membrane. They further pointed out the requirement of the FYVE-like but not the RING domain both for localization of RFFL to the ERC and delayed recycling from the ERC. Therefore, we created a deletion of the FYVE-like domain of RFFL and tested the molecule on co-expressed hERG levels. Just like WT RFFL, RFFL-ΔFYVE co-expression resulted in a robust down-regulation of total hERG (Fig. 2*J*), ruling out the involvement of endosomal recycling in the RFFL-dependent regulation of hERG expression.

Co-immunoprecipitation experiments in 293A cells co-transfected with plasmids allowing the expression of FLAG-tagged RFFL, RFFL-H333A, RFFL-ΔRING, and hERG (Fig. 3*A*) demonstrated an interaction between RFFL or its mutants and the core-glycosylated form of hERG (135 kDa) but not its fully glycosylated form (155 kDa), which is found mainly on the membrane. This interaction implies that RFFL is probably located on the ER and/or possibly the *cis*-Golgi apparatus. Furthermore, we noticed that the RING domain significantly contributed to hERG interaction comparing the amount of co-precipitated hERG with catalytically inactive RFFL-H333A and RFFL-ΔRING lacking the RING domain (Fig. 3, *A* and *B*, *lanes 3* and *4*), which displayed similar levels of expression and immunoprecipitation efficiency. Next, we treated co-transfected 293A cells with 100 nM brefeldin A, a blocker of vesicular transport from the ER to the Golgi apparatus (26). Brefeldin A treatment for 24 h generally resulted in an almost complete disappearance of the fully glycosylated form of hERG and a concomitant increase of its core-glycosylated form (*cf.* 135- and 155-kDa bands in Fig. 3*C*, *lanes 1* and *3*). Importantly, brefeldin A did not prevent RFFL-dependent degradation of hERG (Fig. 3, *C* and *D*) implying that RFFL-dependent degradation of hERG occurs at the endoplasmic reticulum.

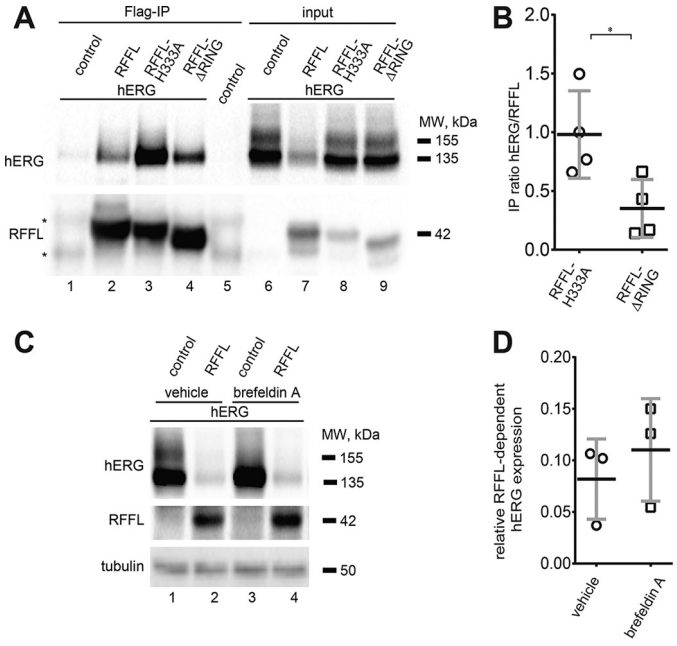

Figure 3. Interaction of RFFL and hERG in 293A cells. *A*, 293A cells were transfected with hERG and FLAG-tagged RFFL, RFFL-H333A, and RFFL-ΔRING expression plasmids or pcDNA3 as control. Co-immunoprecipitation was performed on cell extracts with anti-FLAG antiserum to pulldown RFFL-interacting proteins. A representative immunoblot against hERG protein reveals an interaction between pulled down RFFL or its mutants and core-glycosylated 135-kDa hERG. Input samples were probed against FLAG to detect RFFL and hERG (the *asterisks* indicate unspecific bands). *B*, quantitative analysis on the ratio of co-IP hERG to immunoprecipitated RFFL-H333A, which was set at 1 and hERG to RFFL-ΔRING ($n = 4$ individual co-IP (*, $p < 0.05$)). *C*, RFFL-mediated degradation of hERG occurs at the endoplasmic reticulum. 293A cells were transfected with plasmids for hERG, RFFL, or control plasmid for 24 h and then treated with 100 nM brefeldin A or vehicle for 24 h. Representative Western blotting shows total expression of hERG, RFFL, and tubulin of treated cells. *D*, respective relative expression levels (± S.D.) of total hERG (135- and 155-kDa bands) normalized to α-tubulin levels (three independent experiments performed in triplicate each (*, $p < 0.05$)).

RFFL leads to hERG polyubiquitination and proteosomal degradation in 293A cells

Because RFFL is a member of the RING finger ubiquitin ligase family (14, 27) and several studies (17–19) identified target molecules for ubiquitination by RFFL, we reasoned that RFFL overexpression would result in ubiquitin-mediated degradation of hERG. To this end, we co-transfected expression plasmids for hERG, HA-tagged ubiquitin, FLAG-tagged RFFL, FLAG-tagged RFFL-ΔRING, or control plasmid into 293A cells. Total cell extracts, prepared 48 h later, were immunoprecipitated with anti-HA antibody to enrich for ubiquitinated protein. The ubiquitinated protein fraction was separated by size using SDS-PAGE, transferred to a membrane and probed against hERG. Western blotting data presented in Fig. 4*A* indicate an RFFL-dependent dramatic increase in multiple ubiquitinated hERG bands implying polyubiquitination of hERG. Again, no increase in hERG ubiquitination was noted in cells expressing RFFL void of its catalytic activity. As proteins that are ubiquitinated on the ER get generally degraded via proteasomes (28), we treated cells expressing hERG, RFFL, or control plasmid with the selective proteasome inhibitors MG132 (29) or lactacystin (30) as well as with the lysosomal inhibitor chloroquine (31) for 24 h. Not surprisingly, treatment of cells with MG132 and lactacystin but not chloroquine partially prevented the RFFL-dependent down-regulation of hERG by RFFL (Fig. 4, *B* and *C*). Thus, our data suggest a proteasome-dependent degradation of hERG channel after polyubiquitination by RFFL.

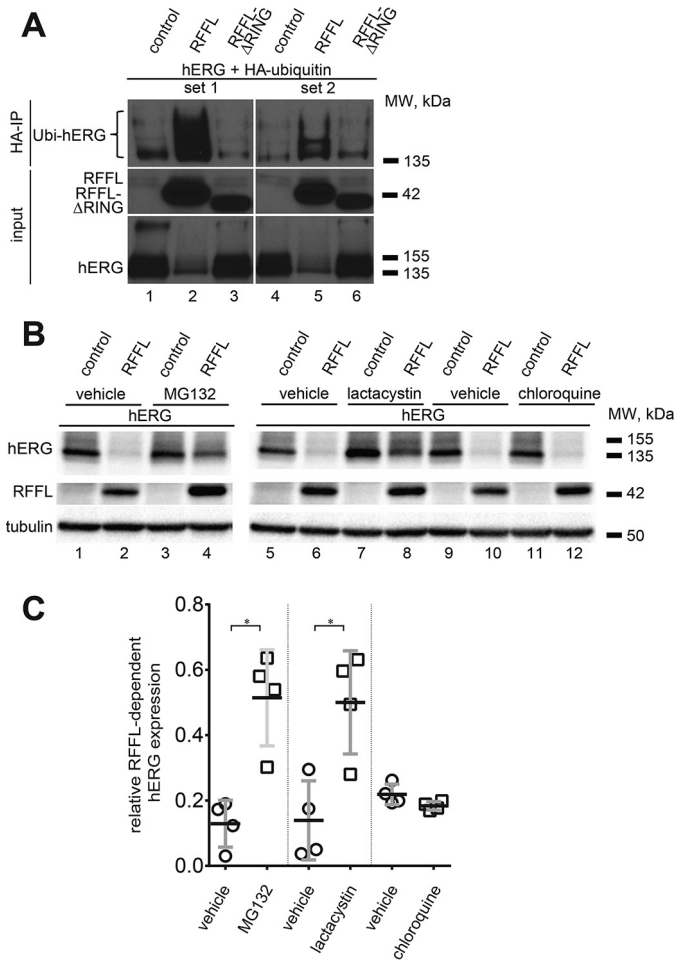

Figure 4. hERG polyubiquitination and proteasomal degradation upon RFFL co-expression in 293A cells. *A*, immunoprecipitation (*IP*) of lysates from 293A cells transfected with plasmids for hERG, HA-tagged ubiquitin, RFFL, RFFL-ΔRING, or plasmid pcDNA3 (control) for 48 h was performed with anti-HA antiserum. A representative immunoblot shows levels of polyubiquitinated hERG and input levels of hERG, FLAG-tagged RFFL, or RFFL-ΔRING. *B*, RFFL-mediated degradation of hERG through proteasomes. 293A cells were transfected with plasmids for hERG, RFFL, or control plasmid for 24 h and then treated with 5 μM MG132, 5 μM lactacystin, 10 μM chloroquine or vehicle for 24 h. Representative Western blots show total expression of hERG, RFFL, and tubulin of treated cells. *C*, respective relative expression levels (± S.D.) of total hERG (135- and 155-kDa bands) normalized to α-tubulin levels (three independent experiments performed in triplicate each (*, $p < 0.05$)).

RFFL-dependent degradation of hERG requires VCP activity

Based on the aforementioned data, hERG polyubiquitination by RFFL is likely happening on the ER. Therefore, it is conceivable that components of the ER-associated degradation (ERAD) pathway are required for RFFL-mediated hERG ubiquitination and degradation. A core component of this pathway is the ATPase valosin-containing protein (VCP), which among other cellular activities is involved in the extraction of ubiquitinated proteins from the ER membrane, a prerequisite for subsequent proteosomal degradation (32). Co-expression of a dominant-negative form of VCP, VCP(DKO), partially blocked hERG degradation by RFFL, whereas WT VCP had no significant effect (Fig. 5, *A* and *B*). Immunoprecipitation experiments (Fig. 5*C*) showed that co-expression of VCP(DKO) and RFFL resulted in a dramatic increase in hERG polyubiquitination compared with RFFL or VCP(DKO) experiments. Finally, we also performed co-immunoprecipitations on protein isolated from 293A cells transiently transfected with expression plasmids for EGFP-tagged VCP (control) or FLAG-tagged RFFL and EGFP-VCP to demonstrate an *in vitro* association between RFFL and VCP (Fig. 5*D*). Data suggest that hERG polyubiquitinated by ER-associated RFFL requires VCP-mediated retrotranslocation prior to proteosomal degradation.

rs2074518 is associated with lower levels of RFFL in the left ventricle of the heart

We used expression quantitative trait loci (eQTL) data from the Genotype-Tissue Expression (GTEx) project (33) to determine whether the SNP rs2074518 (Fig. 6*A*) is associated with *RFFL* expression levels in the heart. Left ventricular heart samples from individuals carrying a heterozygous or homozygous SNP had lower *RFFL* expression (p = 2.3e-6) (Fig. 6*B*). These data suggest that lower levels of RFFL are associated with a shortened QT interval as reported previously (10) and support our findings that RFFL levels affect cardiac repolarization via modifying hERG levels on the membrane.

Discussion

Recent genome-wide association studies (10, 11) of QT interval reported two genetic variants, which are associated with modest changes in QT interval duration (Fig. 6*A*). 1) rs2074518 (10) is located in intron 11 of the DNA ligase 3 (*LIG3*) gene and ~11.7 kb downstream of the *RFFL* gene. 2) rs1052536 (11) is found in the 3′ UTR of the *LIG3* gene and ~4.6 kb downstream of *RFFL*. Furthermore, the chromatin surrounding rs2074518 is characterized by a DNase I hypersensitivity peak cluster, histone H3K27 acetylation, and various transcription factor-binding sites (34–36), all hallmarks of a regulatory region surrounding rs2074518 (Fig. 6*A*). Thus, it is conceivable that genetic variants in this region may indirectly affect expression of nearby genes such as *LIG3* or *RFFL* by altering the chromatin architecture of the aforementioned DNA regulatory region. It is highly unlikely that *LIG3* expression is somewhat linked to the QT interval as it encodes DNA ligase III essential for DNA base-excision in mitochondria (37). By contrast, increased RFFL levels in a congenic rat strain resulted in QT interval shortening, hypertrophy, and hypertension (13). The aforementioned reports prompted us to investigate further the possible link between RFFL and the QT interval. Based on the observed effects of overexpressed RFFL on I_{Kr} in rabbit cardiomyocytes (Fig. 1, *A*–*C*) and hERG polyubiquitination and degradation in 293A cells (Fig. 4), we conclude that RFFL is an important regulator of hERG and thus cardiac repolarization.

Our observations outlined in this study suggest the following model for RFFL (Fig. 7). RFFL binds to and polyubiquitinates immature, core-glycosylated hERG channels on the ER. Polyubiquitination of hERG elicits its proteosomal degradation. Thus, RFFL participates in the ER-associated degradation of hERG. ERAD is an evolutionary conserved pathway to maintain protein homeostasis by degrading misfolded or excess protein (28). Recently, two other ubiquitin ligases, ER-resident CHIP and ER-anchored TRC8, have been reported to participate in ERAD of hERG (38–40). It will be interesting to learn whether these three ubiquitin ligases can act in parallel independently or

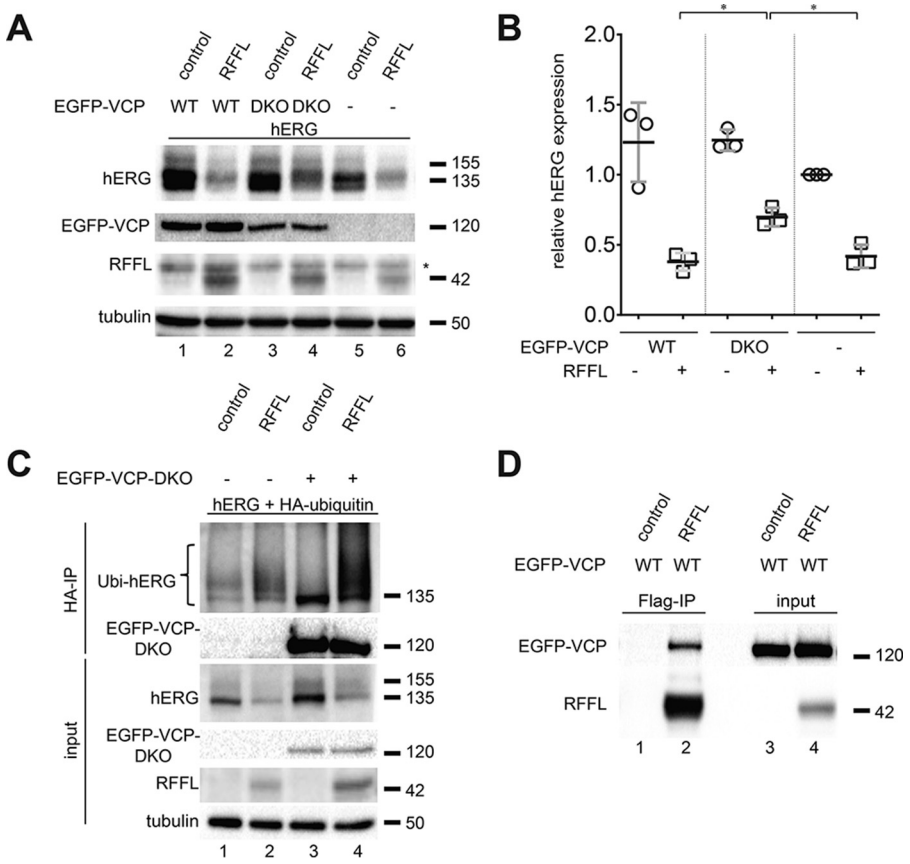

Figure 5. hERG polyubiquitination by RFFL and proteasomal degradation requires VCP in 293A cells. *A*, 293A cells were co-transfected with plasmids for hERG, RFFL, control plasmid, and 300 ng of EGFP-VCP(WT), EGFP-VCP(DKO), or EGFP expression plasmids for 24 h. A representative Western blotting shows total expression of hERG, EGFP-VCP, RFFL, and tubulin of treated cells (the *asterisk* indicates an unspecific band). *B*, respective relative expression levels (± S.D.) of total hERG (135- and 155-kDa bands) in the presence of co-expressed RFFL normalized to α-tubulin levels (three independent experiments performed in triplicate each (*, $p < 0.05$)). *C*, immunoprecipitation (IP) of lysates from 293A cells transfected with plasmids for hERG, HA-tagged ubiquitin, RFFL, EGFP-VCP(DKO), or control plasmid for 24 h was performed with anti-HA antiserum. A representative immunoblot shows levels of polyubiquitinated hERG and input levels of hERG, FLAG-tagged RFFL or EGFP-VCP(DKO). *D*, 293A cells were transfected with EGFP-VCP(WT) and FLAG-tagged RFFL expression plasmids or EGFP as control. Co-IP was performed on cell extracts with anti-FLAG antiserum to pulldown RFFL-interacting proteins. The immunoblot against EGFP protein reveals an interaction between pulled down RFFL and VCP. Input samples were probed against FLAG and GFP to detect RFFL and EGFP-VCP, respectively.

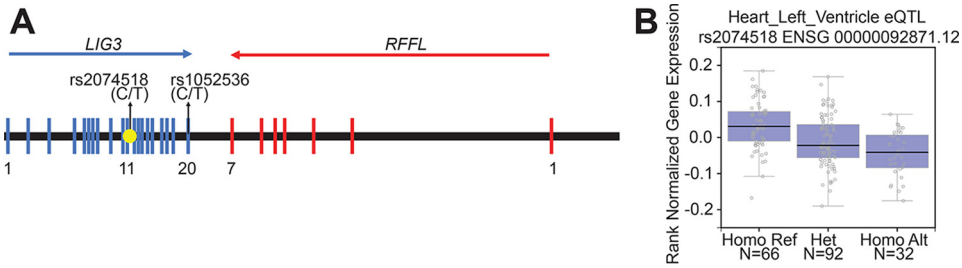

Figure 6. rs2074518 is associated with lower levels of RFFL mRNA in the left ventricle. *A*, schematic of the *RFFL* and *LIG3* gene loci and location of two SNPs associated with QT interval duration (10, 11): rs2074518 is located in intron 11 and rs1052536 in the 3′ UTR of the *LIG3* gene. Exons are represented by *numbered colored rectangles*. The *yellow circle* indicates rs2074518-surrounding chromatin with a DNase I hypersensitivity cluster, histone H3K27 acetylation, and various transcription factor-binding sites, which are based on data from the ENCODE project using various cell lines (34–36). *B*, eQTL data from the GTEx project (33) show that the left ventricular heart samples from individuals carrying a heterozygous or homozygous SNP have lower RFFL mRNA expression ($p = 2.3e\text{-}6$).

in tandem on hERG and identify respective ubiquitination site(s) in the channel. For example, the ubiquitin ligases RMA1 and CHIP act sequentially in the ER membrane and cytosol to monitor the folding status of cystic fibrosis transmembrane conductance regulator (CFTR) and its mutant CFTRΔF508 (41). Similarly, sequential ubiquitination of CFTRΔF508 by RMA1 and gp78 is required for the channel's proteosomal degradation (42). Further studies are also warranted to characterize ERAD proteins required for RFFL-mediated hERG degradation with respect to hERG recognition, retranslocation, ubiquitination, targeting to proteasomes, and degradation (reviewed in Refs. 28 and 43). ERAD is also a crucial part of the ER quality control (ERQC) system (43). A number of studies delineated parts of the ERQC with respect to hERG folding. Transcripts of hERG 1a and 1b are physically associated during translation to provide spatial proximity of nascent proteins required for proper folding and assembly of the channel (44). Also, several (co-) chaperones are required for correct folding

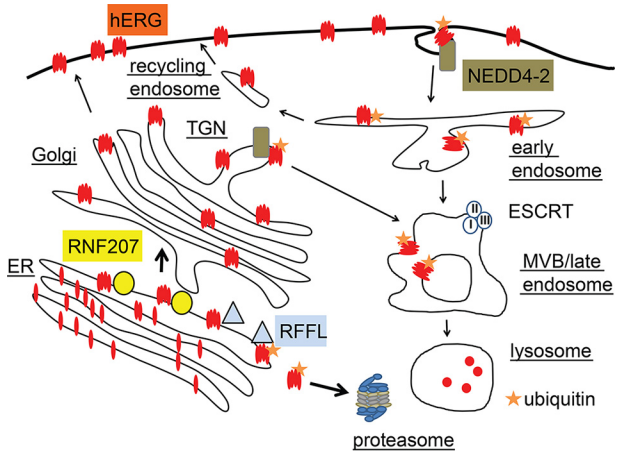

Figure 7. Model of RFFL-mediated degradation of hERG on the ER. RFFL polyubiquitinates hERG on the ER, which leads to proteosomal degradation of the channel. Also depicted are two additional ubiquitin ligases known to target hERG: RNF207 on the ER promotes hERG folding/ER exit/forward trafficking (46); NEDD4-2 located on the trans-Golgi newtwok (*TGN*) (54) as well as cell-surface (55) monoubiquitinates hERG promoting lysosomal hERG degradation. *MVB*, multivesicular body.

of hERG in the ER (reviewed in Ref. 45). Finally, we have recently shown that Ring Finger Protein 207 (RNF207), located on the ER, regulated APD, likely via promoting hERG forward trafficking/folding/ER exit in a heat shock protein-dependent manner (46). It remains to be shown whether RFFL functionally interacts with any of the aforementioned components of the ERQC for hERG.

Okiyoneda *et al.* (47) recently reported that RFFL selectively recognized and polyubiquitinated the unfolded mutant CFTRΔF508 on the plasma membrane. This led to removal of the mutant protein from the membrane and stimulated its lysosomal degradation. The authors suggested that RFFL was crucial in the chaperone-independent peripheral quality control of CFTR. Although our data imply a role for RFFL in ER quality control of hERG, it is plausible that RFFL could also be part of the peripheral quality control of structurally compromised hERG on the plasma membrane. Such a scenario is reminiscent of the ubiquitin ligase CHIP, which is both involved in ERAD of hERG (38–40) as well as in the peripheral quality control of conformationally defective hERG (48).

However, currently, we cannot rule out the possibility that RFFL actually provides hERG quantity rather quality control on the ER. One can envisage that cardiomyocytes must maintain a sufficient number of hERG channels on the membrane required for proper repolarization. In contrast, limiting hERG channels on the cell surface is required to prevent a marked APD shortening underlying short QT syndrome, a risk factor for arrhythmias. For example, the ubiquitin ligase Nrdp1 targets properly folded and functional ErbB3 receptor tyrosine kinase on the ER, which is also dependent on the ERAD pathway ATPase VCP (49). We anticipate that regulatory pathways exist that allow tight control of hERG forward trafficking by regulating stability and/or expression of RFFL. Such pathways could be adversely affected by certain cardiac diseases subsequently impacting I_{Kr}.

Newton-Cheh *et al.* (10) reported that the genetic variant rs2074518 is associated with a modest shortening of the QT interval. Additionally, data from the Genotype-Tissue Expression project (33) indicate that rs2074518 is also associated with lower levels of RFFL transcript in the human left ventricle (Fig. 6*B*). Thus, this correlation between lower RFFL levels and shortened QT interval is strongly supported by our data presented in this study. Here, we show that increased levels of RFFL resulted in lower hERG expression on the membrane reducing I_{Kr}. I_{Kr}, however, is a crucial repolarizing current in large animals (50) and lowering I_{Kr} by certain drugs or a number of hERG mutations is well-known to prolong the QT interval (51). Therefore, RFFL-mediated regulation of hERG-encoded I_{Kr} may well account for the aforementioned association between RFFL levels and QT interval duration. At first sight, such a scenario, *i.e.* increased RFFL levels reduce I_{Kr} and would therefore cause QT interval prolongation, cannot account for the findings by Gopalakrishnan *et al.* (13) who reported that higher levels of RFFL expression resulted in QT interval shortening in a congenic rat strain. However, species-dependent differences in repolarizing voltage-gated potassium currents, *i.e.* transient outward K^+ currents (I_{to}) and delayed, outwardly rectifying K^+ currents (I_K) could explain different effects of RFFL on cardiac repolarization in human or rat. For example, I_{Kr} plays virtually no role in adult rodents (52). In contrast, I_{to} is essential during the whole repolarization phase of the action potential in rodents, whereas in large mammals, including human and rabbit, I_{to} causes only partial membrane repolarization, shaping rapid repolarization of the action potential and setting the height of the initial plateau (53).

Experimental procedures

DNA

Expression plasmids for FLAG-tagged human RFFL (pFLAG-CMV2-CARP2; Addgene ID 16013), HA-tagged ubiquitin-expressing plasmid (pRK5-HA-ubiquitin-WT; Addgene ID 17608), EGFP-tagged WT, and dominant-negative VCP (VCP(WT)-EGFP and VCP(DKO)-EGFP; Addgene IDs 23971 and 23974) were purchased from Addgene. FLAG-tagged RFFL-expressing adenovirus was prepared using the Gateway cloning system (Thermo Fisher Scientific) as described previously (46). The deletions of the RING (ΔRING) and FYVE-like (ΔFYVE) domains as well as the RING domain point mutation H333A were generated by site-directed mutagenesis (46). pcDNA3-hERG and pcDNA3-Kir2.1 express the human hERG and Kir2.1 channels, respectively (25). The plasmid pEGFP was obtained from Clontech.

Transfections

Human embryonic kidney (HEK) 293A cells (Thermo Fisher Scientific), HEK cells stably expressing hERG (25), and U-2 OS cells (ATCC) were cultured in Dulbecco's modified Eagle's medium and split at ~50% confluency. We generally used a 1:1 molar ratio of RFFL and potassium channel expression plasmids (*e.g.* 30 ng of FLAG-tagged RFFL- and 32 ng of hERG-expressing plasmids, 338 ng of pFLAG-CMV-2 (Millipore Sigma) as carrier DNA, and 1.2 μl of Lipofectamine 2000 (Thermo Fisher Scientific) per well of 12-well plates) and incubated the cells for 48 h. The clear-cut effect of RFFL on hERG levels was also seen at lower molar ratios of RFFL and hERG

expression plasmids and at 24 h after transfection (data not shown).

Preparation of rabbit cardiomyocytes

Septal adult rabbit cardiomyocytes (ARbCM) were isolated from the hearts of 6–24–month-old New Zealand White rabbits (both sexes) in accordance with Institutional Animal Care and Use Committee (IACUC)-approved protocols. The filtered cells were maintained in 45 mM KCl, 65 mM potassium glutamate, 3 mM $MgSO_4$, 15 mM KH_2PO_4, 16 mM taurine, 10 mM HEPES, 0.5 mM EGTA, and 10 mM glucose (pH 7.3) for 1 h. Cells were centrifuged, resuspended in medium 199 (Thermo Fisher Scientific) supplemented with 10% FBS (MilliporeSigma), antibiotics, and 0.5 μM cytochalasin D (MilliporeSigma) and plated on laminin-coated cover glasses. After 2–3 h, the medium was replaced and adenovirus (100 m.o.i.) added to the cells. Cells were maintained at 37 °C with 5% CO_2 and ~48 h later, cells were used for patch clamp and biochemistry. Ventricular neonatal rabbit cardiomyocytes (NRbCM) were isolated from 3 to 5-day-old New Zealand White rabbits (both sexes) in accordance with Institutional Animal Care and Use Committee (IACUC)-approved protocols as described previously (23).

Immunoblot analysis

Co-immunoprecipitations and immunoblots were carried out as described in previous studies (25).

Electrophysiological recording

293A cells were transfected with GFP, hERG, and RFFL expression plasmids (or pcDNA3 as control) 48 h before recording. Whole-cell patch clamp recordings of hERG currents were performed with an Axopatch-200B amplifier (Axon Instruments) at room temperature (21–23 °C). Signal was filtered at 1 kHz and analyzed using Origin (Origin Lab). The pipette solution contained 50 mM KCl, 65 mM potassium glutamate, 5 mM $MgCl_2$, 5 mM EGTA, 10 mM HEPES, 5 mM glucose, 5 mM K_2ATP, and 0.25 mM Na_2GTP (pH 7.2). Tyrode solution was used as a standard bath solution and contained 140 mM NaCl, 5.4 mM KCl, 1 mM $CaCl_2$, 1 mM $MgCl_2$, 0.33 mM NaH_2PO_4, 7.5 mM glucose, and 5 mM HEPES (pH 7.4). The whole-cell recordings of transduced (100 m.o.i., 48 h) ARbCM were performed in Tyrode solution. The pipette resistance was 2–4 MΩ when filled with 120 mM KCl, 5 mM $MgCl_2$, 0.36 mM $CaCl_2$, 5 mM EGTA, 5 mM HEPES, 5 mM glucose, 5 mM K_2ATP, 5 mM Na_2CrP, 0.25 mM NaGTP (pH 7.2). I_{Kr} recording started at −40 mV holding potential (HP) followed by a series of 3-s test pulses that were applied in 10-mV increments to maximum membrane potential of +40 mV. Control voltage-clamp recordings were performed at 35 °C in Tyrode solution and then repeated in the same solution with added specific I_{Kr} blocker E-4031 (5 μM; Abcam). Capacitance and 60 to 80% of series resistance were routinely compensated. The sampling frequency was 20 kHz, and −3 dB cut-off frequency was 5 kHz. I_{Kr} amplitude was determined as the peak of E-4031-sensitive tail current after the end of each depolarizing test pulse. The currents were normalized to appropriate cell membrane capacitance and presented as mean ± S.D. Two-way analysis of variance followed by Tukey's post hoc test was used to test for differences in the I-V relationship for normalized peak tail currents.

Author contributions—K. R., C. A. M., and G. K. conceptualization; K. R., A. K., K. S. M., K. R. M., and A. X. data curation; K. R., A. K., K. S. M., K. R. M., A. X., and N. N. T. formal analysis; K. R., A. K., K. S. M., K. R. M., A. X., S. D., C. A. M., and G. K. validation; K. R., K. S. M., K. R. M., A. X., N. N. T., and Y. L. investigation; K. R., A. K., K. S. M., K. R. M., and A. X. visualization; K. R., A. K., K. S. M., K. R. M., A. X., N. N. T., and Y. L. methodology; K. R. and G. K. writing-original draft; K. R., A. K., K. S. M., K. R. M., A. X., S. D., N. N. T., Y. L., C. A. M., and G. K. writing-review and editing; A. K., S. D., C. A. M., and G. K. project administration; S. D. and G. K. resources; S. D., C. A. M., and G. K. supervision; S. D. and G. K. funding acquisition.

Acknowledgments—We are indebted to Drs. Wafik S. El-Deiry (Fox Chase Cancer Center, Department of Hematology/Oncology, Philadelphia, PA) for the RFFL plasmid, Ted Dawson (Johns Hopkins University, Institute for Cell Engineering, Baltimore, MD) for the ubiquitin plasmid, and Nico Dantuma (Karolinska Institutet, Department of Cell and Molecular Biology, Stockholm, Sweden) for the VCP expression plasmids. The data used for the analyses described in this article were obtained (on 10/2/2017) from the GTEx Portal (https://www.gtexportal.org/home/).[4] The Genotype-Tissue Expression (GTEx) Project was supported by the Common Fund of the Office of the Director of the National Institutes of Health, and the NCI, National Human Genome Research Institute (NHGRI), NHLBI, NIDA, NIMH, and NINDS.

References

1. Rautaharju, P. M., Surawicz, B., Gettes, L. S., Bailey, J. J., Childers, R., Deal, B. J., Gorgels, A., Hancock, E. W., Josephson, M., Kligfield, P., Kors, J. A., Macfarlane, P., Mason, J. W., Mirvis, D. M., Okin, P., *et al.* (2009) AHA/ACCF/HRS recommendations for the standardization and interpretation of the electrocardiogram: part IV: the ST segment, T and U waves, and the QT interval: a scientific statement from the American Heart Association Electrocardiography and Arrhythmias Committee, Council on Clinical Cardiology; the American College of Cardiology Foundation; and the Heart Rhythm Society. Endorsed by the International Society for Computerized Electrocardiology. *J. Am. Coll. Cardiol.* **53,** 982–991 CrossRef Medline
2. Mitchell, G. F., Jeron, A., and Koren, G. (1998) Measurement of heart rate and Q-T interval in the conscious mouse. *Am. J. Physiol.* **274,** H747–H751 Medline
3. Seed, W. A., Noble, M. I., Oldershaw, P., Wanless, R. B., Drake-Holland, A. J., Redwood, D., Pugh, S., and Mills, C. (1987) Relation of human cardiac action potential duration to the interval between beats: implications for the validity of rate corrected QT interval (QTc). *Br. Heart J.* **57,** 32–37 CrossRef Medline
4. Tomaselli, G. F., Beuckelmann, D. J., Calkins, H. G., Berger, R. D., Kessler, P. D., Lawrence, J. H., Kass, D., Feldman, A. M., and Marban, E. (1994) Sudden cardiac death in heart failure, the role of abnormal repolarization. *Circulation* **90,** 2534–2539 CrossRef Medline
5. Li, M., and Ramos, L. G. (2017) Drug-induced QT prolongation and torsades de pointes. *P T* **42,** 473–477 Medline
6. Hong, Y., Rautaharju, P. M., Hopkins, P. N., Arnett, D. K., Djoussé, L., Pankow, J. S., Sholinsky, P., Rao, D. C., and Province, M. A. (2001) Familial aggregation of QT-interval variability in a general population: results from

[4] Please note that the JBC is not responsible for the long-term archiving and maintenance of this site or any other third party hosted site.

the NHLBI Family Heart Study. *Clin. Genet.* **59,** 171–177 CrossRef Medline
7. Newton-Cheh, C., Larson, M. G., Corey, D. C., Benjamin, E. J., Herbert, A. G., Levy, D., D'Agostino, R. B., and O'Donnell, C. J. (2005) QT interval is a heritable quantitative trait with evidence of linkage to chromosome 3 in a genome-wide linkage analysis: the Framingham Heart Study. *Heart Rhythm* **2,** 277–284 CrossRef Medline
8. Akylbekova, E. L., Crow, R. S., Johnson, W. D., Buxbaum, S. G., Njemanze, S., Fox, E., Sarpong, D. F., Taylor, H. A., and Newton-Cheh, C. (2009) Clinical correlates and heritability of QT interval duration in blacks: the Jackson Heart Study. *Circ. Arrhythm. Electrophysiol.* **2,** 427–432 CrossRef Medline
9. Pfeufer, A., Sanna, S., Arking, D. E., Müller, M., Gateva, V., Fuchsberger, C., Ehret, G. B., Orrú, M., Pattaro, C., Köttgen, A., Perz, S., Usala, G., Barbalic, M., Li, M., Pütz, B., *et al.* (2009) Common variants at ten loci modulate the QT interval duration in the QTSCD Study. *Nat. Genet.* **41,** 407–414 CrossRef Medline
10. Newton-Cheh, C., Eijgelsheim, M., Rice, K. M., de Bakker, P. I., Yin, X., Estrada, K., Bis, J. C., Marciante, K., Rivadeneira, F., Noseworthy, P. A., Sotoodehnia, N., Smith, N. L., Rotter, J., Kors, J., Witteman, J. C., *et al.* (2009) Common variants at ten loci influence QT interval duration in the QTGEN Study. *Nat. Genet.* **41,** 399–406 CrossRef Medline
11. Arking, D. E., Pulit, S. L., Crotti, L., van der Harst, P., Munroe, P. B., Koopmann, T. T., Sotoodehnia, N., Rossin, E. J., Morley, M., Wang, X., Johnson, A. D., Lundby, A., Gudbjartsson, D. F., Noseworthy, P. A., Eijgelsheim, M., *et al.* (2014) Genetic association study of QT interval highlights role for calcium signaling pathways in myocardial repolarization. *Nat. Genet.* **46,** 826–836 CrossRef Medline
12. Marjamaa, A., Newton-Cheh, C., Porthan, K., Reunanen, A., Lahermo, P., Väänänen, H., Jula, A., Karanko, H., Swan, H., Toivonen, L., Nieminen, M. S., Viitasalo, M., Peltonen, L., Oikarinen, L., Palotie, A., Kontula, K., and Salomaa, V. (2009) Common candidate gene variants are associated with QT interval duration in the general population. *J. Intern. Med.* **265,** 448–458 CrossRef Medline
13. Gopalakrishnan, K., Morgan, E. E., Yerga-Woolwine, S., Farms, P., Kumarasamy, S., Kalinoski, A., Liu, X., Wu, J., Liu, L., and Joe, B. (2011) Augmented rififylin is a risk factor linked to aberrant cardiomyocyte function, short-QT interval and hypertension. *Hypertension* **57,** 764–771 CrossRef Medline
14. Deshaies, R. J., and Joazeiro, C. A. (2009) RING domain E3 ubiquitin ligases. *Annu. Rev. Biochem.* **78,** 399–434 CrossRef Medline
15. Coumailleau, F., Das, V., Alcover, A., Raposo, G., Vandormael-Pournin, S., Le Bras, S., Baldacci, P., Dautry-Varsat, A., Babinet, C., and Cohen-Tannoudji, M. (2004) Over-expression of Rififylin, a new RING finger and FYVE-like domain-containing protein, inhibits recycling from the endocytic recycling compartment. *Mol. Biol. Cell* **15,** 4444–4456 CrossRef Medline
16. Araki, K., Kawamura, M., Suzuki, T., Matsuda, N., Kanbe, D., Ishii, K., Ichikawa, T., Kumanishi, T., Chiba, T., Tanaka, K., and Nawa, H. (2003) A palmitoylated RING finger ubiquitin ligase and its homologue in the brain membranes. *J. Neurochem.* **86,** 749–762 CrossRef Medline
17. Yang, W., Dicker, D. T., Chen, J., and El-Deiry, W. S. (2008) CARPs enhance p53 turnover by degrading 14-3-3σ and stabilizing MDM2. *Cell Cycle* **7,** 670–682 CrossRef Medline
18. Liao, W., Xiao, Q., Tchikov, V., Fujita, K., Yang, W., Wincovitch, S., Garfield, S., Conze, D., El-Deiry, W. S., Schütze, S., and Srinivasula, S. M. (2008) CARP-2 is an endosome-associated ubiquitin ligase for RIP and regulates TNF-induced NF-κB activation. *Curr. Biol.* **18,** 641–649 CrossRef Medline
19. Gan, X., Wang, J., Wang, C., Sommer, E., Kozasa, T., Srinivasula, S., Alessi, D., Offermanns, S., Simon, M. I., and Wu, D. (2012) PRR5L degradation promotes mTORC2-mediated PKC-δ phosphorylation and cell migration downstream of Gα12. *Nat. Cell Biol.* **14,** 686–696 CrossRef Medline
20. Ciechanover, A. (2006) Intracellular protein degradation: from a vague idea thru the lysosome and the ubiquitin-proteasome system and onto human diseases and drug targeting. *Exp. Biol. Med. (Maywood)* **231,** 1197–1211 CrossRef
21. Brunner, M., Peng, X., Liu, G. X., Ren, X. Q., Ziv, O., Choi, B. R., Mathur, R., Hajjiri, M., Odening, K. E., Steinberg, E., Folco, E. J., Pringa, E., Centracchio, J., Macharzina, R. R., *et al.* (2008) Mechanisms of cardiac arrhythmias and sudden death in transgenic rabbits with long QT syndrome. *J. Clin. Invest.* **118,** 2246–2259 Medline
22. Sanguinetti, M. C., and Jurkiewicz, N. K. (1990) Two components of cardiac delayed rectifier K^+ current: differential sensitivity to block by class III antiarrhythmic agents. *J. Gen. Physiol.* **96,** 195–215 CrossRef Medline
23. Organ-Darling, L. E., Vernon, A. N., Giovanniello, J. R., Lu, Y., Moshal, K., Roder, K., Li, W., and Koren, G. (2013) Interactions between hERG and KCNQ1 α-subunits are mediated by their COOH termini and modulated by cAMP. *Am. J. Physiol. Heart Circ. Physiol.* **304,** H589–599 CrossRef Medline
24. McDonald, E. R., 3rd, and El-Deiry, W. S. (2004) Suppression of caspase-8– and −10–associated RING proteins results in sensitization to death ligands and inhibition of tumor cell growth. *Proc. Natl. Acad. Sci. U.S.A.* **101,** 6170–6175 CrossRef Medline
25. Ren, X. Q., Liu, G. X., Organ-Darling, L. E., Zheng, R., Roder, K., Jindal, H. K., Centracchio, J., McDonald, T. V., and Koren, G. (2010) Pore mutants of HERG and KvLQT1 downregulate the reciprocal currents in stable cell lines. *Am. J. Physiol. Heart Circ. Physiol.* **299,** H1525–H1534 CrossRef Medline
26. Klausner, R. D., Donaldson, J. G., and Lippincott-Schwartz, J. (1992) Brefeldin A: insights into the control of membrane traffic and organelle structure. *J. Cell Biol.* **116,** 1071–1080 CrossRef Medline
27. Zheng, N., and Shabek, N. (2017) Ubiquitin ligases: structure, function, and regulation. *Annu. Rev. Biochem.* **86,** 129–157 CrossRef Medline
28. Christianson, J. C., and Ye, Y. (2014) Cleaning up in the endoplasmic reticulum: ubiquitin in charge. *Nat. Struct. Mol. Biol.* **21,** 325–335 CrossRef Medline
29. Tsubuki, S., Saito, Y., Tomioka, M., Ito, H., and Kawashima, S. (1996) Differential inhibition of calpain and proteasome activities by peptidyl aldehydes of di-leucine and tri-leucine. *J. Biochem.* **119,** 572–576 CrossRef Medline
30. Fenteany, G., and Schreiber, S. L. (1998) Lactacystin, proteasome function, and cell fate. *J. Biol. Chem.* **273,** 8545–8548 CrossRef Medline
31. Homewood, C. A., Warhurst, D. C., Peters, W., and Baggaley, V. C. (1972) Lysosomes, pH and the anti-malarial action of chloroquine. *Nature* **235,** 50–52 CrossRef Medline
32. Ye, Y., Meyer, H. H., and Rapoport, T. A. (2001) The AAA ATPase Cdc48/p97 and its partners transport proteins from the ER into the cytosol. *Nature* **414,** 652–656 CrossRef Medline
33. GTEx Consortium (2013) The Genotype-Tissue Expression (GTEx) project. *Nat. Genet.* **45,** 580–585 CrossRef Medline
34. ENCODE Project Consortium (2004) The ENCODE (ENCyclopedia Of DNA Elements) Project. *Science* **306,** 636–640 CrossRef Medline
35. Thomas, D. J., Rosenbloom, K. R., Clawson, H., Hinrichs, A. S., Trumbower, H., Raney, B. J., Karolchik, D., Barber, G. P., Harte, R. A., Hillman-Jackson, J., Kuhn, R. M., Rhead, B. L., Smith, K. E., Thakkapallayil, A., Zweig, A. S., *et al.* (2007) The ENCODE Project at UC Santa Cruz. *Nucleic Acids Res.* **35,** D663–667 CrossRef Medline
36. Farnham, P. J. (2012) Thematic minireview series on results from the ENCODE Project: integrative global analyses of regulatory regions in the human genome. *J. Biol. Chem.* **287,** 30885–30887 CrossRef Medline
37. Simsek, D., Furda, A., Gao, Y., Artus, J., Brunet, E., Hadjantonakis, A. K., Van Houten, B., Shuman, S., McKinnon, P. J., and Jasin, M. (2011) Crucial role for DNA ligase III in mitochondria but not in Xrcc1-dependent repair. *Nature* **471,** 245–248 CrossRef Medline
38. Hantouche, C., Williamson, B., Valinsky, W. C., Solomon, J., Shrier, A., and Young, J. C. (2017) Bag1 co-chaperone promotes TRC8 E3 ligase-dependent degradation of misfolded human ether-a-go-go-related gene (hERG) potassium channels. *J. Biol. Chem.* **292,** 2287–2300 CrossRef Medline
39. Iwai, C., Li, P., Kurata, Y., Hoshikawa, Y., Morikawa, K., Maharani, N., Higaki, K., Sasano, T., Notsu, T., Ishido, Y., Miake, J., Yamamoto, Y., Shirayoshi, Y., Ninomiya, H., Nakai, A., *et al.* (2013) Hsp90 prevents interaction between CHIP and HERG proteins to facilitate maturation of wild-

type and mutant HERG proteins. *Cardiovasc. Res.* **100,** 520–528 CrossRef Medline
40. Walker, V. E., Wong, M. J., Atanasiu, R., Hantouche, C., Young, J. C., and Shrier, A. (2010) Hsp40 chaperones promote degradation of the HERG potassium channel. *J. Biol. Chem.* **285,** 3319–3329 CrossRef Medline
41. Younger, J. M., Chen, L., Ren, H. Y., Rosser, M. F., Turnbull, E. L., Fan, C. Y., Patterson, C., and Cyr, D. M. (2006) Sequential quality-control checkpoints triage misfolded cystic fibrosis transmembrane conductance regulator. *Cell* **126,** 571–582 CrossRef Medline
42. Morito, D., Hirao, K., Oda, Y., Hosokawa, N., Tokunaga, F., Cyr, D. M., Tanaka, K., Iwai, K., and Nagata, K. (2008) Gp78 cooperates with RMA1 in endoplasmic reticulum-associated degradation of CFTRDeltaF508. *Mol. Biol. Cell* **19,** 1328–1336 CrossRef Medline
43. Araki, K., and Nagata, K. (2012) Protein folding and quality control in the ER. *Cold Spring Harb. Perspect. Biol.* **4,** a015438 Medline
44. Liu, F., Jones, D. K., de Lange, W. J., and Robertson, G. A. (2016) Cotranslational association of mRNA encoding subunits of heteromeric ion channels. *Proc. Natl. Acad. Sci. U.S.A.* **113,** 4859–4864 CrossRef Medline
45. Foo, B., Williamson, B., Young, J. C., Lukacs, G., and Shrier, A. (2016) hERG quality control and the long QT syndrome. *J. Physiol.* **594,** 2469–2481 CrossRef Medline
46. Roder, K., Werdich, A. A., Li, W., Liu, M., Kim, T. Y., Organ-Darling, L. E., Moshal, K. S., Hwang, J. M., Lu, Y., Choi, B. R., MacRae, C. A., and Koren, G. (2014) RING finger protein RNF207, a novel regulator of cardiac excitation. *J. Biol. Chem.* **289,** 33730–33740 CrossRef Medline
47. Okiyoneda, T., Veit, G., Sakai, R., Aki, M., Fujihara, T., Higashi, M., Susuki-Miyata, S., Miyata, M., Fukuda, N., Yoshida, A., Xu, H., Apaja, P. M., and Lukacs, G. L. (2018) Chaperone-independent peripheral quality control of CFTR by RFFL E3 ligase. *Dev. Cell* **44,** 694–708.e7 CrossRef Medline
48. Apaja, P. M., Foo, B., Okiyoneda, T., Valinsky, W. C., Barriere, H., Atanasiu, R., Ficker, E., Lukacs, G. L., and Shrier, A. (2013) Ubiquitination-dependent quality control of hERG K+ channel with acquired and inherited conformational defect at the plasma membrane. *Mol. Biol. Cell* **24,** 3787–3804 CrossRef Medline
49. Fry, W. H., Simion, C., Sweeney, C., and Carraway, K. L., 3rd. (2011) Quantity control of the ErbB3 receptor tyrosine kinase at the endoplasmic reticulum. *Mol. Cell. Biol.* **31,** 3009–3018 CrossRef Medline
50. Cheng, J. H., and Kodama, I. (2004) Two components of delayed rectifier K+ current in heart: molecular basis, functional diversity, and contribution to repolarization. *Acta Pharmacol. Sin.* **25,** 137–145 Medline
51. van Noord, C., Eijgelsheim, M., and Stricker, B. H. (2010) Drug- and non-drug-associated QT interval prolongation. *Br. J. Clin. Pharmacol.* **70,** 16–23 CrossRef Medline
52. Xu, H., Guo, W., and Nerbonne, J. M. (1999) Four kinetically distinct depolarization-activated K+ currents in adult mouse ventricular myocytes. *J. Gen. Physiol.* **113,** 661–678 CrossRef Medline
53. Niwa, N., and Nerbonne, J. M. (2010) Molecular determinants of cardiac transient outward potassium current (I(to)) expression and regulation. *J. Mol. Cell. Cardiol.* **48,** 12–25 CrossRef Medline
54. Kang, Y., Guo, J., Yang, T., Li, W., and Zhang, S. (2015) Regulation of the human ether-a-go-go-related gene (hERG) potassium channel by Nedd4 family interacting proteins (Ndfips). *Biochem. J.* **472,** 71–82 CrossRef Medline
55. Guo, J., Wang, T., Li, X., Shallow, H., Yang, T., Li, W., Xu, J., Fridman, M. D., Yang, X., and Zhang, S. (2012) Cell surface expression of human ether-a-go-go-related gene (hERG) channels is regulated by caveolin-3 protein via the ubiquitin ligase Nedd4-2. *J. Biol. Chem.* **287,** 33132–33141 CrossRef Medline